A RANS/EDC Simulation of the Lifted Turbulent Non-Premixed Round Jet of CH_4 Flame

GUESSAB A., ARIS A
Ecole Nationale Polytechnique d'Oran, Oran, ALGERIA

Abstract:— The objectives of this work is to determine the average rate of reaction by numerical study of the reacting flow inside an axisymmetric free jet, and the validation of the eddy dissipation concept (EDC) combustion model implemented in ANSYS Fluent. The validation of the eddy dissipation concept combustion model involved the reproduction of a lifted, non-premixed, turbulent free jet flame described experimentally in Mahmud (2007). Three chemical mechanisms were used along the combustion model, namely the 2-step Westbrook and Dryer mechanism, the skeletal Jones-Lindstedt mechanism and the Hyer mechanism. Turbulence was modeled with the standard k-ε model The flame lift-off height and the temperature profiles are reproduced accurately by the Hyer model.

Keywords:— Standard k-ε model; eddy dissipation concept; reacting flow; flame lift-off

Received: May 23, 2022. Revised: October 24, 2022. Accepted: December 2, 2022. Published: December 31, 2022.

1. Introduction

Numerical simulation is a very important tool in the study of prediction of turbulent reactive flows. Indeed, it has several advantages (gain time, less expensive than the experience....).

Methane is important fuel scientific point of view and for practical application. They are the simplest and best studied. In addition, the physic-chemical description of the oxidation is the base for more complex fuels. CH_4 is not currently used for aerospace propulsion, but it is considered an alternative to H_2 as its calorific value per unit volume is two and a half times greater in the cryogenic state. The characteristics of ignition and combustion of CH_4 can be improved by the addition of H_2 [1]. Interest in CH_4 as fuel has increased significantly over the past five years.

Since methane is the simplest hydrocarbon fuel available; several studies have focused on methane-air flames. The development of the detailed chemical kinetic mechanism for the natural gas combustion began in the 70s, when several high temperature kinetic models for the hydrogen, carbon monoxide and methane oxidation were constructed under the support of a large quantity of experimental data. The oxidation of methane is quite well understood and various detailed reaction mechanisms are reported in literature [2-3].

They can be divided into full mechanisms, skeletal mechanisms, and reduced mechanisms (Tables 1, 2 and 3).

Lifted flames are a challenging problem since the flame at its base is unstable and involves a significant degree of interactions between chemi cal and flow time-scales and can be found in a number of industrial applications (burners and gas turbines). The interactions between chemical and flow time-scales influence stabilization mech anism of these flames which may stabilize at the certain distance from the nozzle or may propa gate and stabilize at the nozzle.

A lifted non-premixed turbulent flame was used to validate the reacting flow module on ANSYS Fluent v. 15. The code computes the reaction rates directly from the chemistry mechanism, and uses a turbulence/chemistry interaction model, Eddy dissipation concept, the EDC model, to resolve the turbulent flame structure.

The reference work for this validation is the flame studied experimentally and numerically by [4]. It consists of a free jet methane flame discharging into still air through a burner with an inner diameter, Djet, of 5 mm. In flame measurements of gas temperature and NO concentration are presented in the reference work and compared with the presented results computed with ANSYS Fluent v. 15.

TABLE I. LIST OF GLOBAL MECHANISM

Mechanism	Fuel	NO_x	No. of species	Number of steps	Ref.
GRI-Mech v.1.2	Gas natural	non	32	177	[5]
GRI-Mech v.3.0	Gas natural	oui	53	325	[6]
Konnov v.1.5	CH_4-C_3H_8	oui	127	1207	[7]
LCSR	Gas natural	oui	101	618	[8]
Leeds v.1.5	CH_4-C_2H_6	non	37	175	[9]
CERMECH	CH_4-C_3H_8	non	39	173	[10]

TABLE II. LIST OF REDUCED MECHANISM

Mechanism	No. of species		Number of steps	
	Total	without NO_x	Total	without NO_x
Revel [11]	10	8	6	5
Jiang [12]	8	8	5	5
Kundu (12 espèces) [13]	12	9	13	9
Kundu (16 espèces) [13]	16	12	23	15

TABLE III. LIST OF SKELETAL MECHANISM

Author	Designation	Species	Number of steps	Ref.
Kazakov and Frenklach	DRM19	19	84	[14]
Kazakov and Frenklach	DRM22	22	104	[14]

Yungster and Rabinowitz	Yungster	19	52	[15]
Petersen and Hanson	REDRAM	21	35	[16]
Li and Williams	Li	16	24	[17]
MFC5	MFC	9	5	[18]
MFC9	ARM9 (Flient)	9	9	[19]
ARM2	ARM19 (Fluent)	19	19	[20]
12 step GRI2.11	12 step GRI2.11	16	12	[21]
13 step GRI3	13 step GRI3	17	13	[21]
10 step GRI2.11	10 step GRI2.11	14	10	[22], [23]
8 step GRI 12	8 step GRI 12	12	8	[24]
6 step GRI 12	6 step GRI 12	10	6	[24]

2. The Governing Equations

2.1 Problem Description

Figure 1 is a schematic of the burner. The fuel free jet, which has an inner diameter D = 5 mm. An experimental and numerical results study of lifted flame was reported by [24]. Figure 1 illustrates the axisymmetric numerical domain enclosing the turbulent flame structure. The computational domain is an axisymmetric plane with symmetry axis coincident with the axis of the burner.. The total pressure of the combustor is 94 KPa. In the fuel stream, the uniform inlet gas velocity is 46.4 m/s, with a temperature of 293K. In the air stream, the uniform inlet air velocity is 0.8 m/s, with a preheated temperature of 293K. The outlet boundary is located at 200Djet from burner exit and the entrainement boundary, parallel to the symmetry axis, is placed at $50D_{jet}$ from the axis.

2.2 Mathematical models

A prediction ANSYS Fluent code for turbulent reacting flows includes submodels describing flow field, combustion, and heat transfer by radiation. In their entirety, the different submodels form a system of strongly coupled partial differential equations. Each of these equations can be written in the form of a general transport equation:

$$\frac{\partial}{\partial x}(\rho U \Phi) = \frac{\partial}{\partial x}\left(\Gamma \frac{\partial \Phi}{\partial x}\right) + S_{\Phi} \qquad (1)$$

where ρ, u, x, S_{Φ} and Γ are density, velocity, coordinates, source term, and diffusion coefficient, respectively. This equation describes the local change of the Favre-averaged variable Φ caused by convection, diffusion, and production on Φ, Eq. (1) represents mass, momentum, species, or energy conservation.

Fig. 1. Axisymmetric numerical model geometry

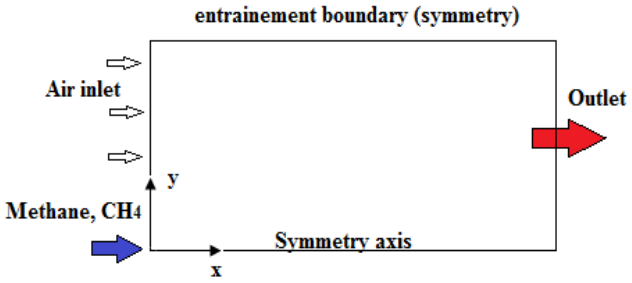

The Navier-Stokes equations are solved for the primitive variables with a Standard k-ε turbulence closure. Atransport equation, Eq. (1), is solved for the mean mass fraction of each balanced species. The mass density is determined by the ideal gas equation od state. Thermal radiation is modeled using the discrete transfer method proposed by ANSYS Fluent.

2.3 Eddy Dissipation Concept Model (EDC)

In this study, the Eddy Dissipation Concept (EDC) is used to model the influence of turbulence on chemical reactions. With the EDC, it is possible to include a detailed reaction mechanism in turbulent flame calculations. The presented EDC combined with chemical kinetics is a general concept that allows inclusion of radiation, fuel generated by particles, and the simulation of multiple inlets with different fuel compositions. The Eddy-dissipation Concept model is an extension of the eddy-dissipation model to include detailed chemical mechanisms in turbulent flows. It assumes that the reactions occur in small turbulent structures, called the fine scales. The length fraction of the fine scales is modeled as [25]:

$$\xi^{*} = 2.1377\left(\frac{\nu\varepsilon}{k^2}\right)^{1/4} \qquad (2)$$

Where $(*)$ denotes fine-scale quantities and ν kinematic viscosity. In the EDC the total space is subdivided into a reaction space, called the 'fine structures' and the 'surrounding fluid'. All reactions of the gas phase components are assumed to take place within this reaction space which represents the smallest turbulence scales where all turbulent energy is dissipated into heat. All reactions in the surrounding fluid are neglected. Thus in order to be able to treat the reactions within the fine structures, the volume fraction of the reaction space g* and the mass transfer rate M* between the fine structures and the surrounding fluid have to be determined.

$$M^{*} = 2.45\left(\frac{\varepsilon}{\nu}\right)^{1/2} \qquad (3)$$

Both quantities are derived from the turbulence behavior of the fluid. The expression for mean chemical source term in

the transport equation for the mean mass fraction $\widetilde{Y}_i$, is obtained as:

$$\widetilde{R}_i = \frac{\overline{\rho}\left(\xi^{\bullet}\right)^2}{\tau^{\bullet}\left[1-\left(\xi^{\bullet}\right)^3\right]}\left(Y_i^{\bullet}-\widetilde{Y}_i\right) \quad (4)$$

where $Y_i^{\bullet}$ is the fine-scale species mass fraction after reacting over the time.

$$\tau^{\bullet}\ (=0.4082\left(\nu/\varepsilon\right)^{0.5}) \quad (5)$$

The EDC model can incorporate detailed mechanisms into turbulent reacting flows. Details of the applied Eddy dissipation concept (EDC) implementation are given in [26].

Chemical kinetic mechanisms of oxidation of methane

The two following mechanisms are investigated: The Westbrook and Dryer mechanism (WD) [27]. consists of two reactions, where the 2nd step, oxidation of CO to CO_2, is reversible. Table 1 shows the rates equations. The rate constant for the 1st and 2nd reactions originate from [28], in which high-temperature oxidation of CO and CH_4 was studied under fuel lean conditions in a turbulent flow reactor. Later, Westbrook and Dryer [27] included the reverse reaction step for CO_2 decomposition in order to reproduce the proper heat of reaction and pressure dependence of the [CO]/[CO2] equilibrium.

TABLE IV. WESTBROOK AND DRYER MECHANISM (2-STEP)

WD1	$CH_4+1.5O_2 \rightarrow CO_2+2H_2O$
WD2	$CO+0.5O_2 \rightarrow CO_2$
WD3	$CO_2 \rightarrow CO+0.5O_2$

The Jones and Lindstedt mechanism: the 4-step global mechanisms developed by [28] for the combustion of alkane hydrocarbons up to butane in mixtures with air in premixed and diffusion flames. The schemes include two competing fuel breakdown reactions, and equilibrium assumptions have been used to derive initial estimates of the forms of the rate expressions. The reduced four-step reaction mechanism is,

TABLE V. THE JONES- LINDSTEDT MECHANISM (4-STEP)

JL1	$CH_4+0.5O_2 \rightarrow CO+2H_2$
JL2	$CH_4+H_2O \rightarrow CO+3H_2$
JL3f	$H_2+0.5O_2 \rightarrow H_2O$
JL3r	$H_2O \rightarrow H_2+0.5O_2$
JL4	$CO+H_2O \leftrightarrow CO_2+H_2$ (forward)

TABLE VI. RATES EQUATIONS OF THE ORIGINAL WESTBROOK AND DRYER MECHANISM: UNITS IN [M], [S], [KMOL], [J] AND [K]

Eq.	Rates equations [Kmol/(m^3.s)]
WD1	$\frac{d[CH_4]}{dt} = 5.012\times10^{11}e^{-2.0\times10^8/(RT)}.[CH_4]^{0.7}[O_2]^{0.8}$
WD2	$\frac{d[CO]}{dt} = 2.239\times10^{12}e^{-1.7\times10^8/(RT)}.[CO][O_2]^{0.25}[H_2O]^{0.5}$
WD3	$\frac{d[CO_2]}{dt} = 5\times10^8e^{-1.7\times10^8/(RT)}.[CO_2]$

TABLE VII. RATES EQUATIONS OF THE ORIGINAL JONES-LINDSTEDT MECHANISM: UNITS IN [M], [S], [KMOL], [J] AND [K]

Eq.	Rates equations [Kmol/(m^3.s)]
JL1	$\frac{d[CH_4]}{dt} = 4.4\times10^{11}e^{-1.26\times10^8/(RT)}.[CH_4]^{0.5}[O_2]^{1.25}$
JL2	$\frac{d[CH_4]}{dt} = 3.0\times10^8e^{-1.7\times10^8/(RT)}.[CH_4][H_2O]$
JL3f	$\frac{d[H_2]}{dt} = 6.8\times10^{15}T^{-1}e^{-1.67\times10^8/(RT)}.[H_2]^{0.25}[O_2]^{1.5}$
JL3r	$\frac{d[H_2O]}{dt} = 1.255\times10^{17}T^{-0.877}e^{-4.095\times10^8/(RT)}.[H_2]^{-0.75}[O_2][H_2O]$
JL4	$\frac{d[CO]}{dt} = 2.75\times10^9e^{-8.4\times10^7/(RT)}.[CO][H_2O]$

The Hyer mechanism: rates equations of the The reaction mechanism adopted in this work contains 8 chemical species (CH_4, CO_2, H_2O, O_2, CO, H_2, C_2H_6 and N_2 as inert) and 8 reactions of Hyer (Table VIII) [29]. The formation of NO_x is not taken into account. This mechanism was successfully utilized, in previous work of [30].

TABLE VIII. ORIGINAL HYER MECHANISM: UNITS IN [M], [S], [KMOL], [J] AND [K]

Reaction	A_k	E_k [*j/Kmol*]	β_k
$CH_4+0.5O_2 \rightarrow CO+2H_2$	4.40e+09	1.26e+08	0
$CH_4+H_2O \rightarrow CO+3H_2$	3.00e+08	1.26e+08	0
$CO+H_2O \rightarrow CO_2+H_2$	2.75e+10	8.37e+07	0
$CO_2+H_2 \rightarrow CO+H_2O$	9.62e+10	1.26e+08	-0.85
$H_2+0.5O_2 \rightarrow H_2O$	7.45e+13	1.67e+08	-0.91
$H_2O \rightarrow H_2+0.5O_2$	3.83e+14	4.12e+08	-1.05
$C_2H_6+O_2 \rightarrow 2CO+3H_2$	4.20e+11	1.25e+08	0
$C_2H_6+2H_2O \rightarrow 2CO+5H_2$	3.00e+08	1.25e+08	0

NO_X FORMATION

There are two mechanisms that create NOx in a gas turbine combustor: the Thermal NOx, which is the oxidation of atmospheric bound nitrogen in the combustion air and the conversion of fuel bound nitrogen into NOx. The formation of thermal NOx is determined by a set of highly temperature-dependent chemical reactions known as the extended Zeldovich mechanism. The principal reactions governing the formation of thermal NOx from molecular nitrogen are as follows [31]:

$$O + N_2 \Leftrightarrow N + NO \quad (6)$$

$$N + O_2 \Leftrightarrow O + NO \quad (7)$$

A third reaction has been shown to contribute to the formation of thermal NOx, particularly at near-stoichiometric conditions and in fuel-rich mixtures:

$$N + OH \Leftrightarrow H + NO \quad (8)$$

The expressions for the rate coefficients for Equs. 6, 7 and 8 used in the NO_x model are given below. These were selected based on the evaluation of [25].

$$K_{f,1} = 1.8 \times 10^8 \exp\{-38370/T\} \quad (9)$$

$$K_{r,1} = 3.8 \times 10^7 \exp\{-425/T\} \quad (10)$$

$$K_{f,2} = 1.8 \times 10^4 \, T \exp\{-4680/T\} \quad (11)$$

$$k_{r,2} = 3.81 \times 10^3 \, T \exp\{-20820/T\} \quad (12)$$

$$k_{f,3} = 7.1 \times 10^7 \exp\{-450/T\} \quad (13)$$

$$k_{r,3} = 1.7 \times 10^8 \exp\{-24560/T\} \quad (14)$$

In the above expressions, $k_{f,1}$, $k_{f,2}$, and $k_{f,3}$ are the rate constants for the forward reactions Equs. 9, 11 and 13, respectively, and $k_{r,1}$, $k_{r,2}$, and $k_{r,3}$ are the corresponding reverse rate constants. All of these rate constants have units of m^3/mol-s. The net rate of formation of NO via the reactions in Equation 6, 7 and 8 is given by

$$\frac{d[NO]}{dt} = k_{f,1}[O][N_2] + k_{f,2}[N][O_2] + k_{f,3}[N][OH] - k_{r,1}[NO][N] - k_{r,2}[NO][O] - k_{r,3}[NO][H] \quad (15)$$

where all concentrations have units of mol/m^3.

To determine the O radical concentration, ANSYS Fluent uses one of three approaches – the equilibrium approach, the partial equilibrium approach, and the predicted concentration approach. This study uses the equilibrium approach. The kinetics of the thermal NO_x formation rate is much slower than the main hydrocarbon oxidation rate, and so most of the thermal NO_x is formed after completion of combustion. Therefore, the thermal NO_x formation process can often be decoupled from the main combustion reaction mechanism and the NO_x formation rate can be calculated by assuming equilibration of the combustion reactions. Using this approach, the calculation of the thermal NO_x formation rate is considerably simplified. The assumption of equilibrium can be justified by a reduction in the importance of radical overshoots at higher flame temperature. According to [32], the equilibrium O-atom concentration can be obtained from the expression

$$[O] = 3.97 \times 10^5 T^{-1/2} [O_2]^{1/2} e^{-31090/T} \quad [mol/m^3] \quad (16)$$

ANSYS Fluent uses one of three approaches to determine the OH radical concentration of OH from the thermal NO_x calculation approach, the partial equilibrium approach, and the use of the predicted OH concentration approach. In this study, we used the partial equilibrium approach, in this approach, the concentration of OH in the third reaction in the extended Zeldovich mechanism (Eq. 8) is given by:

$$[OH] = 2.129 \times 10^2 T^{-0.57} e^{-4595/T} [O]^{1/2} [H_2O]^{1/2} \quad (17)$$

The presence of a second mechanism leading to NO_x formation was first identified by [33] and was termed "Prompt NO_x ". There is good evidence that prompt NOx can be formed in a significant quantity in some combustion environments, such as in low-temperature, fuel-rich conditions and where residence times are short. Surface burners, staged combustion systems, and gas turbines can create such conditions. At present, the prompt NO_x contribution to total NO_x from stationary combustion is small. However, as NO_x emissions are reduced to very low levels by employing new strategies (burner design or furnace geometry modification), the relative importance of the prompt NO_x can be expected to increase. More information can be found in ANSYS help. In turbulent combustion calculations, ANSYS Fluent solves the density-weighted time-averaged Navier-Stokes equations for temperature, velocity, and species concentrations or mean mixture fraction and variance. To calculate concentration, a time-averaged formation rate must be computed at each point in the domain using the averaged flow-field information. Methods of modeling the mean turbulent reaction rate can be based on either moment methods or probability density function (PDF) techniques. ANSYS FLUENT uses the PDF approach.

TURBULENCE MODELING

The standard k-ε model (including a correction for round jets performed by using the Pope formulation) turbulence closure model is adopted. In the *k-ε* model the Reynolds stress is closed using mean velocity gradients employing Boussinesq hypothesis. In the case of a jet flame, a correction is necessary to accurately predict the spreading rate of the jet. This is performed by using the Pope correction, P_{pc}, as an additional term in the equation of turbulence dissipation rate (ε) [25]:

$$P_{PC} = \bar{\rho} C_{\varepsilon 3} \frac{\varepsilon^2}{k} S_\varepsilon \quad (18)$$

The term S_ε can be written as (Pope, 1978)[38]:

$$S_\varepsilon = \omega_{ij} \omega_{jk} S_{ij} \quad (19)$$

$$S_{ij} = \frac{1}{2} \frac{k}{\varepsilon} \left(\frac{\partial u_i}{\partial x_j} + \frac{\partial u_j}{\partial x_i} \right) \quad (20)$$

$$\omega_{ij} = \frac{1}{2} \frac{k}{\varepsilon} \left(\frac{\partial u_i}{\partial x_j} - \frac{\partial u_j}{\partial x_i} \right) \quad (21)$$

Where: $C_{\varepsilon 3}$ = 0.79, the standard model constants have been chosen. As an option in the formulation of the k-ε model, enhanced wall functions were selected in accordance with the grid design. This option ensured that appropriate modeling occurred to resolve the viscous sub-layer.

Results and Discussion

In this section, numerical results are presented and a comparison with the measurements of Mahmud *et al.* [4] is made. the flame lifted-off is discussed. A lifted turbulent flame calculation with full chemistry needs a large amount of CPU time consumed by the solution of a nonlinear equation system to determine the source terms of the species. We begin by comparing the computational cost of the three kinetic models in terms of the average CPU (execution) time per time step. The relative elapsed CPU times are compared in Table IX.

TABLE IX. Average execution time per time step

Scheme	species	reaction	CPU	Nb. iterations
2-step	**5**	**2**	0.00885	796
4-step	6	4	0.3589	3456
8-stem	7	8	1.2036	43569

In the 8-step mechanism, more reaction equations are computed, then more CPU time is spent and more difficult it is to convergence. That in general the computational cost increases with the number of reaction-step and species and more difficult it is to convergence. Figure 2 shows a contour plot of mean temperature in the flame. The flame temperature begins to exceed the pilot temperature of the co-flow (1045K) at ≈ h (x/D), which means that the calculated flame lift-off heigh h_{EDC} is about 10 times of the jet diameter. the reported experimental flame lift-off height is near h = 0.127. The flame lift-off is calculated accurately by the model and the adopted Hyer reaction mechanism for CH_4 (Table X). The radial profiles of temperature are shown in Figs. 4, 5 and 6. From the temperature profiles, it can be seen clearly that there are two regions in the flame, including the pure mixing region (x<0.04) and the burnt region (x>0.04). In the pure mixing, the cold fuel from the fuel jet is not ignited by the hot coflow and only mixes, so the temperature in this region does not exceed the coflow temperature. However, in the burnt region, the fuel and the oxidant are mixed to some extent and are ignited. The predicted temperature agree with the measurements well. At x = 0.5m., the predicted peak temperature is a bit higher than the measurement, while at x = 0.6m, 0.7m, the predicted peak temperature is a bit lower than the measured one. Overall, the estimated temperature distribution obtained with the Westbrook and Dryer (2-step) scheme and the JL (4-step) scheme were fairly similar over the entire numerical domain, with only residual differences, whereas the solution with the Hyer (8-step) mechanism although also similar near the burner to the solution of the other chemical mechanisms (Figs. 4 and 5), exhibited a temperature decay in the trailing region of the flame, as observed in the temperature contours and profiles presented. Moreover, the temperature contours on Fig. 2 show that a non-reacting region near the symmetry axis penetrates into the flame and pushes the flame front near the axis further downstream. As evidenced in the axial profiles along the symmetry axis of Figure 3, the maximum penetration distance measured in the numerical solutions is roughly between 0.2 and 0.4 m from the burner, depending slightly on the chemical scheme used. Unfortunately, the experimental data available is not enough to locate the maximum penetration of this non reacting region. In Figs. 4, 5 and 6, both the numerical predictions and measurements at station x = 0.2 m are consistent with the previous observations, showing the extended non reacting region for y < 0.02 m, while in the region 0.02 < y < 0.07 m the high temperature gradients indicate the development of the reacting flow. At stations x = 0.2m and x= 0.4m in Fig. 5 and Fig. 6, the temperature profiles are appreciably higher than the experimental data. At station x = 0.7m, the flame core temperature decreases due to the heat flux from the hot burnt gases to the surrounding air, overcoming the combustion heat release. However, the Westbrook and Dryer and Jones-Lindstedt mechanisms do not differ much in predicting the general methane combustion progress. The full mechanism of WD, JL and Hyer is used to calculate nitrogen oxide. The predicted axial profile agrees well with the available mesurements (see Fig. 10). Unfortunately, no data are available beyound an axial distance of 0.71m, which would allow a complete validation. In Fig. 10, the NO concentration profile is underpredicted. Following an idea of Mahmud et al. [4], the fraction of thermal NO is investigated by deleting the Prompt NO initiation reactions. As evidenced in Fig. 9, the temperatures considerably high above 1600K, estimated with the Hyer chemical mechanism, triggered the intense formation of thermal-NO at the flame front. In addition, the inadequacy of the eddy dissipation concept (EDC) model in determining the reaction rates also contributed to the significant over-prediction of NO relatively to the experimental results. The NO is then transported downstream by the flow to the trailing region of the flame. At location x = 0.7, as oxygen becomes available, the incoming NO is re-oxidized, producing NO, as illustrated by the dashed-blue line in the plot of Figure 10. Because both oxidations of the atmospheric nitrogen are highly endothermic reactions, it is reasonable to admit that the flame temperature decay is due to energy (heat) consumption of the chemical oxidation reactions producing NO.

Fig. 2. Contour plot of temperature

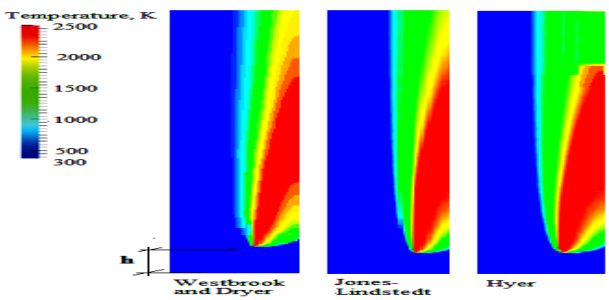

TABLE X. LIFT-OFF HEIGHTS MEASURED FROM THE NUMERICAL RESULTS AND DETERMINED FROM THE EXPERIMENTAL DATA

Westbrook and Dryer	Jones and Lindstedt	Hyer	Exp. data [Mahmud, 2007]
h = 0.1315	0.131	0.129	0.127

Fig. 3. Predicted and measured axial profiles of the mean gas temperature

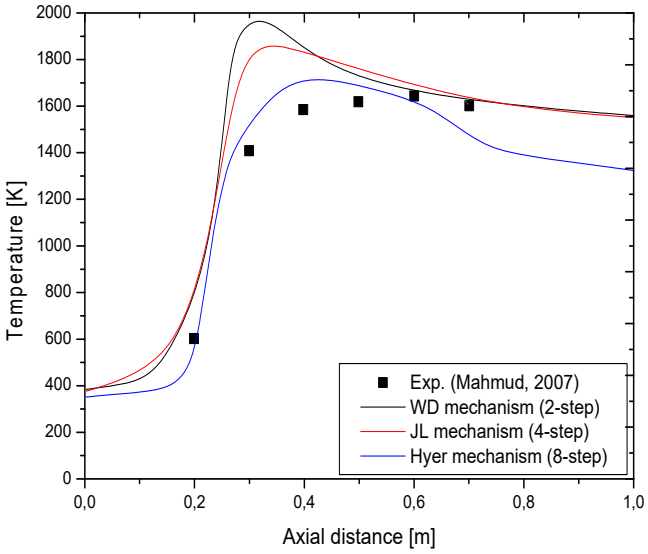

Fig. 4. Predicted and measured radial profiles of the mean gas temperature at x = 0.2m stations along the length of the flame

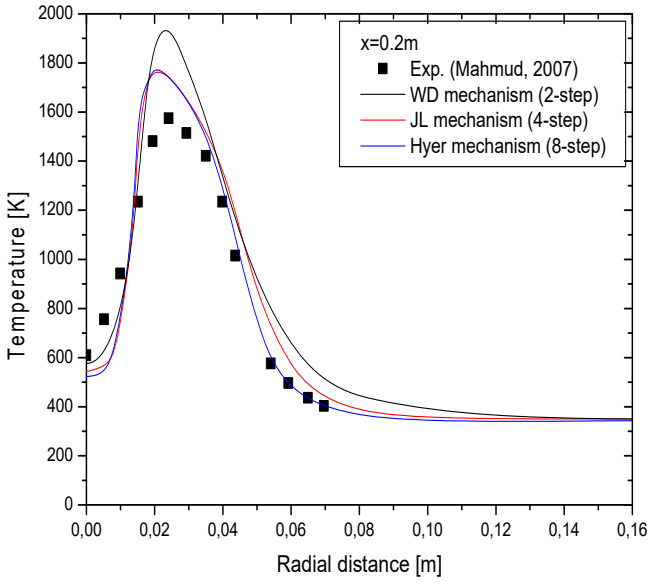

Fig. 5. Predicted and measured radial profiles of the mean gas temperature at x = 0.3m stations along the length of the flame

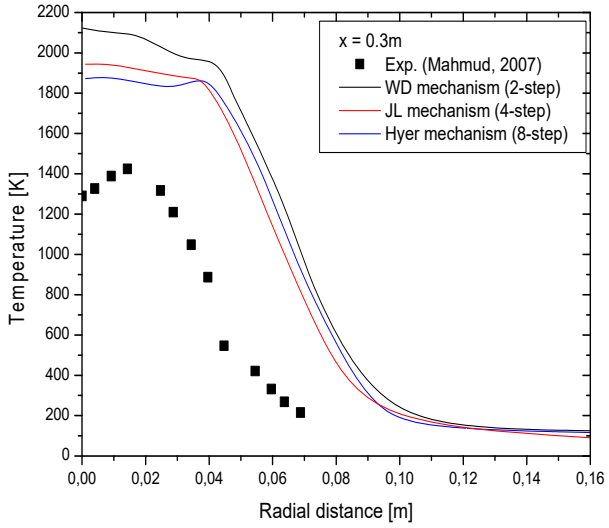

Fig. 6. Predicted and measured radial profiles of the mean gas temperature at x = 0.4m stations along the length of the flame

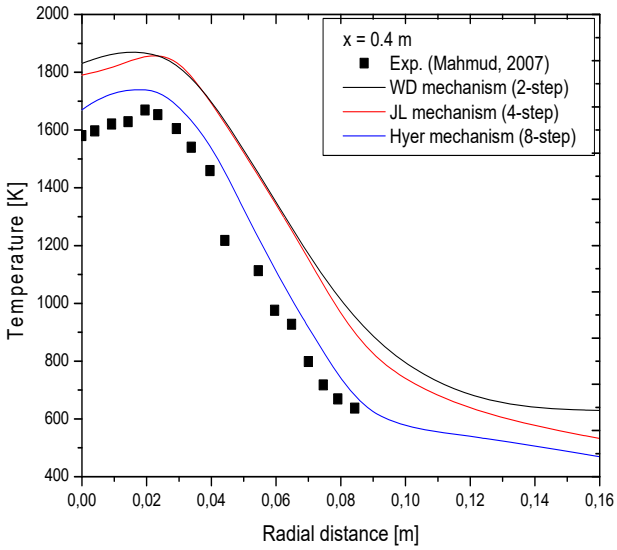

Fig. 7. Predicted and measured radial profiles of the mean gas temperature at x = 0.5m stations along the length of the flame

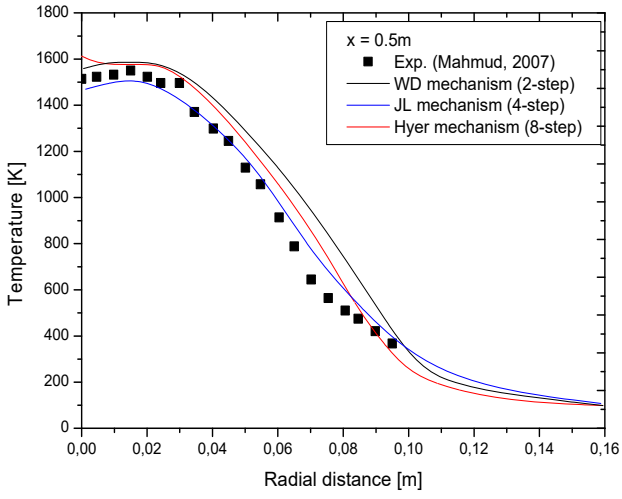

Fig. 8. Predicted and measured radial profiles of the mean gas temperature at x = 0.6m stations along the length of the flame

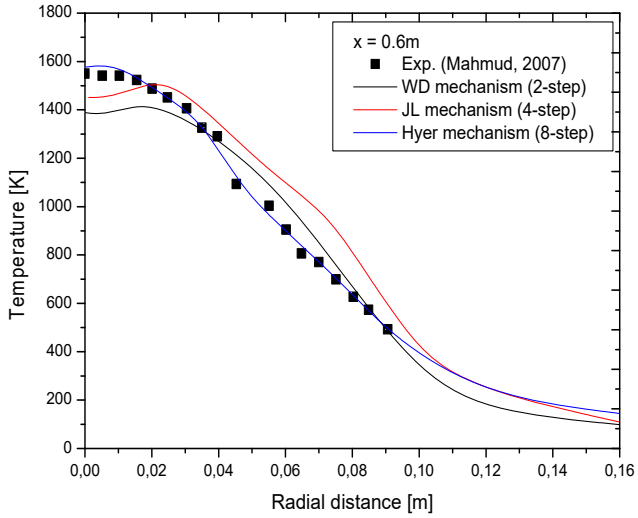

Fig. 9. Predicted and measured radial profiles of the mean gas temperature at x = 0.7m stations along the length of the flame

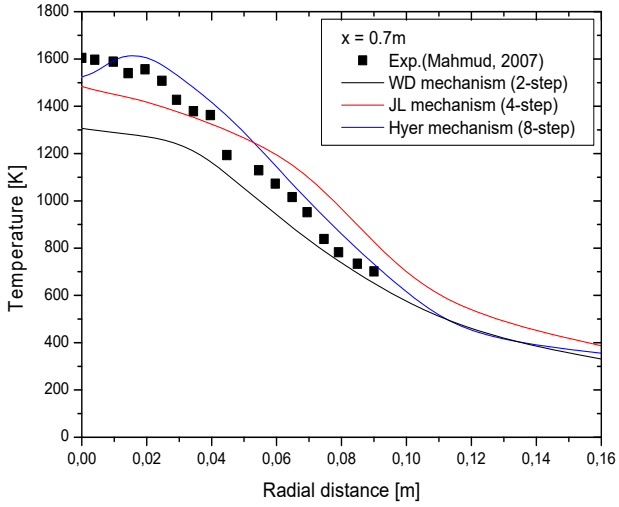

Fig. 10. Axial profiles of NO concentration

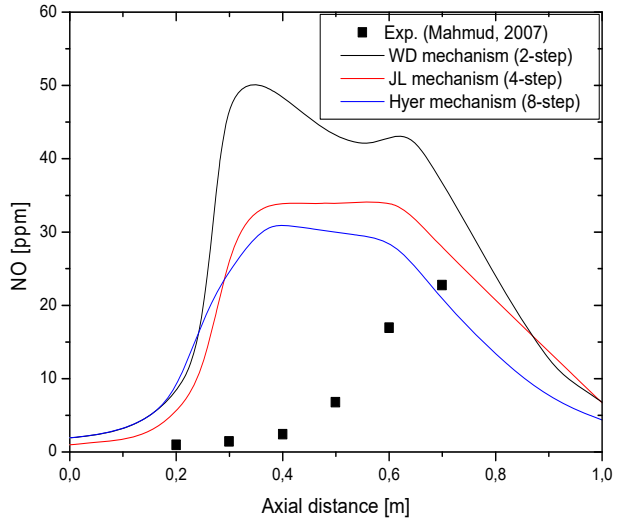

3. Conclusion

A combustion model capable of representing detailed chemical reaction mechanisms in the framework of a turbulent combustor flow simulation on an eddy dissipation concept has been investigated. From the simulation of the lifted Turbulent non-premixed flame of methane, the following main results have been obtained:

- An two step, four-step and eight species methane oxidation mechanism derived from WD, JL and Hyer was successfully implanted into the ANSYS Fluent. The precompiled mechanism was linked to the solver by the means of user defined function (UDF).
- Prediction with Hyer reaction mechanism gives good agreement with measured temperature data.
- Using the Eddy Dissipation Concept (EDC), it is possible to apply steady-state conditions inside the fine structure.

References

[1] A. Guessab, A. Aris, A. Bounif and I. Gokalp, " Numerical Analysis of Confined Laminar Diffusion Flame: Effects of Chemical Kinetics Mechanisms". International Journal Of Advanced Research in Engineering and Technology (IJARET), Vol. 4, pp. 59-78 (2013). www.iaeme.com/ijaret.asp

[2] A. Guessab, A. Aris,F. Tabet Helal and I. Gokalp, " Effect of the Variation of the Mixing Coefficient on a Turbulent Confined CH_4/Air Flame". Journal Communication Science and Technology (COST)-2013.

[3] D. M. Davidenko,I. Gökalp, E. Dufour and P. Magre, "Numerical simulation of supersonic combustion with CH_4-H_2 fuel, European Conference for Aerospace Sciences (EUCASS), Moscow, Russia, 4-7 July (2005).

[4] T. Mahmud, S. K. Sangha, M. Costa & A. Santos," Experimental and computational study of a lifted, non-premixed turbulent free jet flame. FUEL , 86, 793-806, (2007).

[5] M. Frenklach, H. Wang, C-L. Yu, M. Goldenberg, C. T. Bowman, R. K. Hanson, D. F. Davidson, E. J. Chang , G. P. Smith, D. M. Golden, W. C. Gardiner and V. Lissianski, http://diesel.me.berkeley.edu/~gri_mech/new21/version12/text12.html

[6] G. P. Smith, D. M. Golden, M. Frenklach , N. W. Moriarty, B. Eiteneer , M. Goldenberg , C. T. Bowman , R. K. Hanson, S. Song, W. C. Gardiner, V. V. Lissianski and Z. Qin, http://www.me.berkeley.edu/gri_mech/version30/text30.html

[7] A. Konnov, "Detailed reaction mechanism for small hydrocarbons combustion", http://homepages.vub.ac.be/~akonnov/science/mechanism/main.html#refer

[8] P. Dagaut," On the kinetics of hydrocarbon oxidation from natural gas to kerosene and diesel fuel", Phys.Chem. Chem. Phys., Vol. 4, p. 2079–2094 (2009).

[9] Leeds NOx Mechanism, http://www.chem.leeds.ac.uk/Combustion/nox.htm

[10] San Diego Mechanism 2003/08/30,http://maemail.ucsd.edu/~combustion/cermech/olderversions/sandiego20030830/

[11] J. Revel, J. C. Boettner, M. Cathonnet, J. C. Bachman, "Derivation of a global chemical kinetic mechanism for methane ignition and combustion", *Journal de Chimie Physique*, Vol. 91, p. 365-382 (1984).

[12] B. Jiang, D. Ingram, D. Causon and R. Saunders, "A global simulation method for obtaining reduced reaction mechanisms for use in reactive blast flows", *Shock Waves*, Vol. 5, p. 81-88 (1995).

[13] K. P. Kundu, P. F. Penko and S.-L. Yang, "Reduced reaction mechanisms for numerical calculations in combustion of hydrocarbon fuels", AIAA-98-0803, 36th Aerospace Sciences Meeting and Exibit, Reno, NV, 12-15 January (1998).

[14] A. Kazakov, M. Frenklach, "Reduced Reaction Sets based on GRI-Mech 1.2" ,http://www.me.berkeley.edu/drm/

[15] S. Yungster and M. J. Rabinowitz, "Computation of shock-induced combustion using a detailed methane-air mechanism", Journal of Propulsion and Power, Vol. 10, No. 5, p. 609-617 (1995).

[16] E. L. Petersen and R. K. Hanson, "Reduced kinetics mechanisms for ram accelerator combustion", Journal of Propulsion and Power, Vol. 15, No. 4, p. 591-600 (1999).

[17] S. C. Li and F. A. Williams, "Reaction mechanisms for methane ignition", Journal of Engineering for Gas Turbines andPower, Vol. 124, p. 471-480(2002).

[18] H. P. Mallampalli, T. H. Fletcher and J.-Y. Chen, Paper 96F-098, Presented at the Fall Meeting of the Western States Section of the Combustion Institute, University of Southern California, Los Angeles, CA, October 28-29, 1996

[19] C. J. Sung, C. K. Law and J. Y. Chen, Proceedings of the Combustion Institute, Vol. 27, pp 295-304, (1998)

[20] Available online at http://www.ca.sandia.gov/TNF/chemistry.html (Last accessed August 2007)

[21] Available online at http://firebrand.me.berkeley.edu/ (Last accessed August 2007)

[22] J. Y. Chen, Workshop on 'Numerical Aspects of Reduction in Chemical Kinetics', CERMICS-ENPC Cite Descartes - Champus sur Marne, France, September 2nd, (1997)

[23] W.-C. Chang and J.-Y. Chen, http://firebrand.me.berkeley.edu/griredu.html (Last accessed August 2007)

[24] SMITH, G. P., D. M. Golden, M. Frenklach , N. W. Moriarty, B. Eiteneer , M. Goldenberg , C. T. Bowman , R. K. Hanson, S. Song, W. C. Gardiner, V. V. Lissianski and Z. Qin, http://www.me.berkeley.edu/gri_mech/version30/text30.html

[25] Ansys Fluent 14.0, Theory guid. http://www.ansys.com

[26] B. F. Magnussen, "The eddy dissipation concept: a bridge between science and technology," in Proceedings of the ECCOMAS Thematic Conference on Computational Combustion,2005.

[27] C. K. Westbrook, F. L. Dryer, "Simplified reac-tion mechanisms for the oxidation of hydrocarbon fuels in flames", Combustion Sciences and Technologies 27(1-2): 31-43 (1981). http://dx.doi.org/10.1080/00102208108946970.

[28] W. P. Jones and R. P. Lindstedt, "Global reaction schemes for hydrocarbon combustion", Combustion and Flame 73(3): 233-249.
http://dx.doi.org/10.1016/0010-2180(88)90021-1.

[29] P. Hyer, D. Stocker and I. O. Clar, "Gravitational Effects on Laminar Diffusion Flames", Creare. X Users' Group Meeting Proceedings, 345-372 (1981).

[30] A. Guessab, A. Aris and A. Bounif, "Simulation of Turbulent Piloted Methane Non-premixed Flame based on Combination of Finite-Rate/Eddy-DissipationMmodel". ISSN 1392-1207. Mechanika. Vol. 19 (6). pp. 657-664 (2013).
cross[ref] http://dx.doi.org/10.5755/j01.mesh.19.6.6000

[31] S. M. Palash, M. A. kalam, H. H. Masjuki, I. M. Rizwanul Fattah and M. Mofijur, "Impact of biodiesel Combustion on NOx emissions and their reduction approaches". J. Renewable and Sustainably Energy reviews, vol. 23, p. 473-490(2013). http://umexpert.um.edu.my/filepublication/00003184_92278.pdf

[32] A. A. Westenberg , (2009). Comb. Sci. Tech.. vol. 4,p. 59.

[33] J. Zeldovich, "The oxidation of nitrogen in combustion explosions". Acta Physico-chim. U.R.S.S., vol. 21, p. 577-628(1946).

Guessab Ahmed was born in Algeria, Planteurs City, Oran, in 1974. He received his Bachelor degree in mathematics from Ibn Badiss School, Oran. Engineer degree in Mechanical Engineering from Oran University Algeria (USTOMB) in 2002, and he has Magister Degrees, in energetic from mechanical institute Oran University (USTOMB) in 2004. He was a teacher of some disciplines in National Polytechnic School from 2005 to present day. He focuses his research interests on the turbulent flow, models of turbulent combustion and combustion CFD simulation.

Aris Abdelkader is an Assistant Professor of Mechanical Engineering at the National Polytechnic School of Oran, Algeria. He received his Ph.D in Mechanical Engineering from Oran University, USTO.MB (Algeria) in 2006. His researches focus on numerical and experimental combustion phenomenon (internal combustion engine, burners and furnaces), heat transfer and renewable energy. He is responsible for the team's energy specialty in engineering school (ENP.Oran)